

# Supporting Information

## Decrease of protein vicinal dithiols in Parkinsonism disclosed by a mono-arsenical fluorescent probe

Guodong Hu<sup>a</sup>, Huiyi Jia<sup>a</sup>, Yanan Hou<sup>a</sup>, Xiao Han<sup>a</sup>, Lu Gan<sup>b</sup>, Jing Si<sup>b</sup>, Dong-Hyung Cho<sup>c</sup>, Hong Zhang<sup>\*b</sup>, Jianguo Fang<sup>\*a</sup>.

<sup>a</sup> State Key Laboratory of Applied Organic Chemistry and College of Chemistry and Chemical Engineering, Lanzhou University, Lanzhou, Gansu 730000, China.

<sup>b</sup> Department of Heavy Ion Radiation Medicine, Institute of Modern Physics, Chinese Academy of Sciences, 509 Nanchang Road, Lanzhou, Gansu 730000, China.

<sup>c</sup> School of Life Sciences, Kyungpook National University, 80 Daehakro Bukgu, Daegu 41566, Republic of Korea.

\*Corresponding author,

(J. Fang) E-mail: fangjg@lzu.edu.cn

(H. Zhang) E-mail: zhangh@impcas.ac.cn

### CONTENTS

#### 1 Materials and Methods

#### 2 Experiment results

**Figure S1** Time-dependent fluorescent response of **NEP** towards rBSA.

**Figure S2** Time-dependent fluorescent response of **NPP** towards rBSA.

**Figure S3** Time-dependent fluorescent response of **NCC** towards rBSA.

**Figure S4** Dose-dependent emission spectra of **NEP** with the increasing concentrations of rBSA.

**Figure S5** Time course of the fold of fluorescence intensity increment of **NEP** in

the presence of different concentrations of rBSA.

**Figure S6** Time course of the fold of fluorescence intensity increment of **NEP** in the presence of DMPS.

**Figure S7** HPLC analysis of the reaction of **NEP** and DMPS.

**Table S1.** HPLC analysis of the conversion of **NEP** reduced by DMPS

**Figure S8** ESI-MS analysis of the reaction of **NEP** and DMPS.

**Figure S9** LC-MS analysis of the reaction of **NPP** and DMPS.

**Figure S10** Time course of the fold of fluorescence intensity increment of **NEP** in the presence of different concentrations of reduced *E. Coli* Trx.

**Figure S11** Inorganic salt, common amino acids and hydrogen peroxide were reacted with **NEP**.

**Figure S12** low molecular weight dithiols compounds were reacted with **NEP**.

**Figure S13** Cytotoxicity of **NEP**.

**Figure S14** HepG2 cells were incubated with **NEP** for different times.

**Figure S15** Fluorescence co-localization assay.

**Figure S16** The reaction of **NEP** and 6-OHDA

**Figure S17** The fluorescent response of **NEP** and rBSA in the presence of different concentrations of 6-OHDA.

**Figure S18-S39.** <sup>1</sup>H NMR, <sup>13</sup>C NMR and HRMS spectrum of **NEP**, **NPP**, **NCC**.

### **3 References.**

## 1. Materials and methods

### 1.1 Reagents and instruments

The recombinant U498C thioredoxin reductase mutant (Sec→Cys) was produced as described<sup>1</sup>. The PC12 cells and HepG2 cells were obtained from the Shanghai Institute of Biochemistry and Cell Biology, Chinese Academy of Sciences. Dulbecco's modified Eagle's medium (DMEM), reduced glutathione (GSH), dimethyl sulfoxide (DMSO), human serum albumin (HSA), 3-(4, 5-dimethylthiazol-2-yl)-2, 5-diphenyltetrazolium bromide (MTT), 2, 3-dimercaptopropanesulfonic sodium (DMPS), dithiothreitol (DTT) were obtained from Sigma-Aldrich (St. Louis, MO, USA). 6-hydroxydopamine (6-OHDA) was from Santa Cruz Biotechnology. Fetal bovine serum (FBS) was obtained from Sijiqing (Hangzhou, China). Bovine serum albumin (BSA) was obtained from Beyotime (Nantong, China). Human Trx1 and the recombinant *E. coli* Trx was prepared according to our published procedures<sup>2</sup>.

Dichloromethane (DCM) and toluene were respectively distilled from calcium hydride and sodium. N, N-dimethyl formamide (DMF) was distilled from reduced pressure distillation. 2-(4-aminophenyl) ethanol, 2-(7-Azabenzotriazol-1-yl)-N, N, N', N'-tetramethyluronium hexafluorophosphate (HATU), N, N-diisopropyl-ethylamin (DIPEA), triphosgene were purchased from commercial sources and used as received without further purification. <sup>1</sup>H NMR and <sup>13</sup>C NMR spectra were measured on a Bruker AVANCE III 400 NMR spectrometer using CDCl<sub>3</sub> (tetramethylsilane as the internal standard), DMSO-d<sub>6</sub> as solvent. MS spectra were recorded on Bruker Daltonics esquire 6000 mass spectrometer and Shimadzu LCMS-2020. The cell fluorescence imaging was performed with a Fluid cell imaging station microscope.

HPLC was recorder on Shimadzu LCMS-2020 system with a Wondasil C18 Superb reversed-phase column (5  $\mu\text{m}$ , 4.6  $\times$  150  $\mu\text{m}$ ). The fluorescence images of zebrafish were taken with a fluorescence microscope (Olympus BX51, Japan). The fluorescence co-localization assay was performed with the DeltaVision Elite Deconvolution/TIRF microscope system from Applied Precision (GE Healthcare).

### *1.2 Synthesis of the probe **NPP** and the control probe **NCC***

4-aminophenylarsenoxide, 1,3-dimercapto-2-propanol, N-Boc-3-aminopropanoic acid and **Nap-NH<sub>2</sub>** were synthesized according to the references <sup>2,3</sup>.

#### *1.2.1 Synthesis of compound 2*

4-aminophenylarsenoxide (2.0 mmol, 368 mg) was dissolved in 30 mL anhydrous ethanol, and then 1, 3-dimercapto-2-propanol (2.2 mmol, 274 mg) was added in the solution. The reaction system was reflux for 2 h and the colour of reaction turn clear. After the solvent was removed under reduced pressure, and the residue was purified by column chromatography (petroleum ether: acetone = 3:1) to give a white solid (364 mg, 63% yield). <sup>1</sup>H NMR (400 MHz, CDCl<sub>3</sub>)  $\delta$ : 7.61 (d,  $J$  = 8.4 Hz, 2H), 6.74 (d,  $J$  = 8.4 Hz, 2H), 3.98-3.90 (m, 3H), 3.069-3.03 (m, 2H), 2.87 (dd,  $J$  = 14.0, 7.2 Hz, 2H). <sup>13</sup>C NMR (100 MHz, DMSO-d<sub>6</sub>)  $\delta$ : 148.82, 133.99, 132.75, 120.13, 114.78, 114.00, 68.25, 34.73, 31.18.

#### *1.2.2 Synthesis of compound 4*

This compound was prepared in a manner similar to synthesis of compound **3**

(Yield: 54%).  $^1\text{H}$  NMR (400 MHz,  $\text{CDCl}_3$ )  $\delta$ : 8.41 (s, 1H), 7.86-7.77 (m, 2H), 7.71-7.64 (m, 2H), 5.25 (s, 1H), 3.94 (s, 1H), 3.49-3.45 (m, 2H), 2.88 (t,  $J$  = 11.4 Hz, 2H), 2.71-2.61 (m, 5H), 1.43 (s, 9H).  $^{13}\text{C}$  NMR (100 MHz,  $\text{DMSO-d}_6$ )  $\delta$ : 169.85, 155.65, 151.19, 140.10, 139.70, 134.72, 133.28, 132.57, 130.42, 128.94, 120.79, 119.94, 119.43, 77.72, 68.19, 31.19, 28.32. ESI-MS ( $m/z$ ):  $[\text{M}+\text{Na}]^+$  483.00.

### 1.2.3 Synthesis of compound **5**

This compound was prepared in a manner similar to synthesis of compound **3** (Yield: 70%).  $^1\text{H}$  NMR (400 MHz,  $\text{CDCl}_3$ )  $\delta$ : 7.74 (s, 1H), 7.45 (d,  $J$  = 8.4 Hz, 2H), 7.17 (d,  $J$  = 8.4 Hz, 2H), 5.18 (s, 1H), 3.84 (t,  $J$  = 6.4 Hz, 2H), 3.49 (s, 2H), 2.83 (t,  $J$  = 6.6 Hz, 2H), 2.59 (t,  $J$  = 5.8 Hz, 2H), 1.43 (s, 3H).  $^{13}\text{C}$  NMR (100 MHz,  $\text{DMSO-d}_6$ )  $\delta$ : 169.28, 155.65, 151.14, 139.71, 137.20, 134.72, 134.25, 129.03, 128.89, 120.75, 119.16, 77.71, 62.39, 38.56, 36.81, 36.66, 28.28. ESI-MS ( $m/z$ ):  $[\text{M}+\text{Na}]^+$  331.0.

### 1.2.4 Synthesis of compound **NPP**

This compound was prepared in a manner similar to synthesis of **NEP** (Yield: 28%).  $^1\text{H}$  NMR (400 MHz,  $\text{DMSO-d}_6$ )  $\delta$ : 8.70-8.59 (m, 1H), 8.50-8.40 (m, 2H), 8.13 (dd,  $J$  = 10.8, 8.4 Hz, 1H), 7.81-7.73 (m, 5H), 4.97-4.95 (m, 1H), 4.02-3.98 (m, 2H), 3.18-3.11 (m, 2H), 3.02 (d,  $J$  = 11.2 Hz, 1H), 2.88-2.84 (m, 2H), 2.60 (t,  $J$  = 6.4 Hz, 1H), 2.46-2.42 (m, 2H), 1.60-1.56 (m, 2H), 1.35-1.30 (m, 2H), 0.92 (t,  $J$  = 7.2 Hz, 3H).  $^{13}\text{C}$  NMR (100 MHz,  $\text{DMSO-d}_6$ )  $\delta$ : 170.93, 163.43, 162.83, 153.42, 152.77, 141.24, 140.25, 133.14, 132.77, 131.66, 130.78, 130.07, 129.90, 129.20, 128.26,

126.13, 123.82, 122.05, 119.98, 119.48, 117.77, 116.46, 72.14, 37.97, 29.70, 28.32, 19.88, 13.79. HRMS (ESI) calculated for  $[C_{29}H_{32}O_5N_4AsS_2]^+$   $[M+H]^+$  requires  $m/z = 655.1025$ , found 655.1006.

### 1.2.5 Synthesis of compound **NCC**

This compound was prepared in a manner similar to synthesis of **NEP** (Yield: 40%).  $^1H$  NMR (400 MHz, DMSO- $d_6$ )  $\delta$ : 8.67 (d,  $J = 8.0$  Hz, 1H), 8.50-8.43 (m, 2H), 8.10 (d,  $J = 8.4$  Hz, 1H), 7.81 (t,  $J = 4.2$  Hz, 1H), 7.54 (d,  $J = 8.4$  Hz, 2H), 7.24 (d,  $J = 8.4$  Hz, 2H), 4.36 (t,  $J = 7.0$  Hz, 2H), 4.04 (t,  $J = 7.4$  Hz, 2H), 2.95 (t,  $J = 6.8$  Hz, 2H), 2.83 (t,  $J = 6.6$  Hz, 2H), 2.37 (t,  $J = 6.6$  Hz, 2H), 1.65-1.57 (m, 2H), 1.40-1.30 (m, 2H), 0.92 (t,  $J = 7.4$  Hz, 3H).  $^{13}C$  NMR (100 MHz, DMSO- $d_6$ )  $\delta$ : 169.29, 163.42, 162.87, 155.56, 154.01, 140.71, 137.64, 134.16, 132.46, 131.55, 130.83, 129.30, 129.11, 128.92, 128.27, 126.27, 123.92, 122.15, 119.24, 119.07, 118.37, 117.03, 77.62, 65.66, 62.28, 36.75, 36.56, 34.14, 29.67, 28.22, 19.80, 13.69. HRMS (ESI) calculated for  $[C_{28}H_{31}O_5N_4]^+$   $[M+H]^+$  requires  $m/z = 503.2289$ , found 503.2283.

### 1.3 Preparation of mutant thioredoxin.<sup>2,4,5</sup>

The pET-28a-*E. Coli* Trx plasmid was used as a template to construct mutant Trx plasmid by a site-directed mutagenesis procedure via extension of overlapping gene segments by polymerase chain reaction (PCR). The following primers were used as mutagenic primers (C35A, 5'-GATTTCTGGGCAGAGTGGTGCGGTCCGGCCAAAATGATCGCCCCGATT C-3',

5'-GAATCGGGGCGATCATTTTGGCCGGACCGCACCACTCTGCCCAGAAAT  
 C-3';) and flanking primers  
 (5'-GTGCCGCGCGGCAGCCATATGAGCGATAAAATTATTCACC-3',  
 5'-GGTGGTGGTGGTGGTGGTCTCGAGTTACGCCAGGTTAGCGTCGAGGAACT  
 CTTTC-3') to generate mutant *E. Coli* Trx. NdeI and XhoI sites were introduced at  
 the 5' and 3' ends. Final product was inserted into NdeI- XhoI -digested pET-28a  
 vector to generate larger quantities of DNA. The pET-28a-C35A *E. Coli* Trx was  
 transformed into *E. coli* Rosetta cells using the heat shock method. And the  
 recombinant Trx was expressed as fusion proteins containing six histidine residues  
 and was induced in logarithmic cultures of *E. coli* by the addition of 1.5 mM  
 isopropyl  $\beta$ -Dthiogalactopyranoside (IPTG). After 8 hours, bacteria were centrifuged  
 and lysed under nondenaturing conditions. Thioredoxin was purified by using a  
 Ni-NTA (Sangon biotech).

#### *1.4 Cell culture and cytotoxic activity assay.*

HepG2 cells and PC12 cells were cultured in DMEM supplemented with 2 mM  
 glutamine, 10% FBS, and 100 units mL<sup>-1</sup> penicillin/streptomycin and maintained in  
 an atmosphere of 5% CO<sub>2</sub> at 37 °C. Cells were incubated with probe **NEP** (0, 1, 2, 5,  
 10, 15, 20, and 30  $\mu$ M) in triplicate in a 96-well plate for 2 h or 8 h at 37 °C. After the  
 treatment, 10  $\mu$ L MTT (5 mg/mL) was added and incubated for an additional 4 h at  
 37 °C. 100  $\mu$ L extraction buffer (10% SDS, 5% isobutanol, 0.1% HCl) was added,  
 and the cells were incubated overnight at 37 °C. The absorbance was measured at 570  
 nm on Multiskan GO (Thermo Scientific).

### *1.5 Zebrafishes fluorescence imaging<sup>6</sup>*

The collected 4-day-old zebrafishes were washed using standard zebrafish E3 culture medium, and then incubated with probe **NEP** (10  $\mu$ M) for 4 h at 28 °C in the E3 culture medium. For control experiments, the zebrafishes were incubated with probe **NCC** (10  $\mu$ M) for 4 h at 28 °C. After that, the larvae were washed three times with E3 culture medium, and then anaesthetized by using 0.01% ethyl 3-aminobenzoate methanesulfonate (Sigma, USA). The fluorescence images were taken with a fluorescence microscope (Olympus BX51, Japan) at  $\times 40$  magnification.

### *1.6 HPLC Analyses of the Reaction between **NEP** and DMPS*

Probe **NEP** (20  $\mu$ M) was incubated with DMPS (2 mM) in PBS buffer (10 mM, pH 7.4) at 37 °C for 1 h. All samples were passed through a 0.22  $\mu$ m filter, and 20  $\mu$ L of sample was loaded onto the liquid chromatograph. The mixture of methanol and water (7:3, v/v) was used as eluent at the flow rate of 0.6 mL min<sup>-1</sup>. The detection wavelength for **NEP** and compound **Nap-NH<sub>2</sub>** respectively was set at 366 nm and 425 nm.

## 2. Experiment results

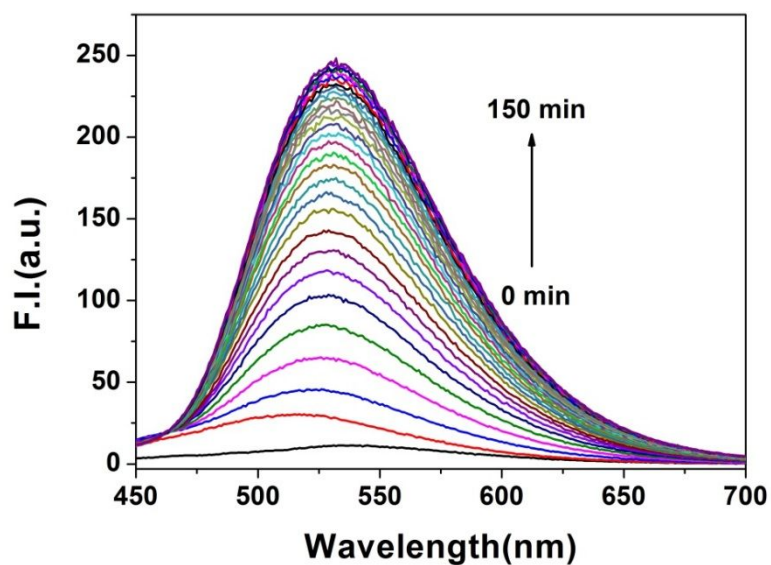


**Figure S1** Time-dependent fluorescent response of **NEP** (10  $\mu\text{M}$ ) towards rBSA (10  $\mu\text{M}$ ) in PBS buffer (10 mM, pH 7.4). All fluorescence spectra were obtained with the excitation at 425 nm.

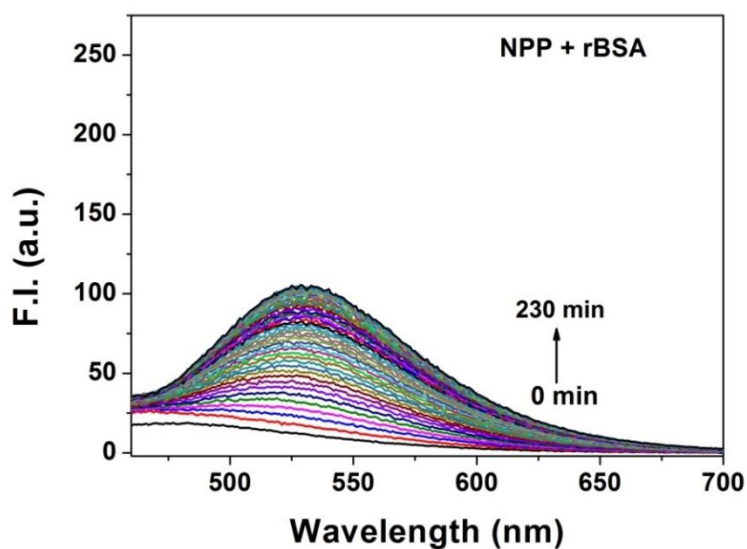


**Figure S2** Time-dependent fluorescent response of **NPP** (10  $\mu\text{M}$ ) towards rBSA (10  $\mu\text{M}$ ) in PBS buffer (10 mM, pH 7.4). All fluorescence spectra were obtained with the excitation at 425 nm.

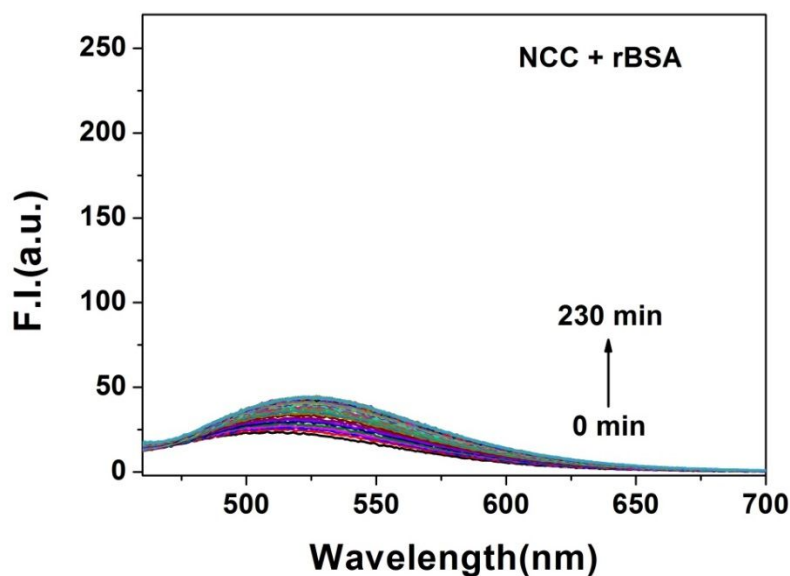


**Figure S3** Time-dependent fluorescent response of NCC (10  $\mu\text{M}$ ) towards rBSA (10  $\mu\text{M}$ ) in PBS buffer (10 mM, pH 7.4). All fluorescence spectra were obtained with the excitation at 425 nm.

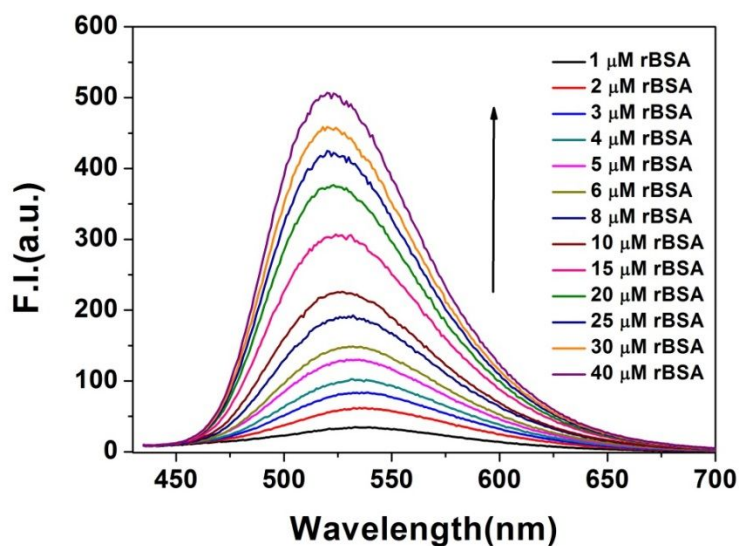


**Figure S4** Dose-dependent emission spectra of NEP (10  $\mu\text{M}$ ) with the increasing concentrations of rBSA (1-40  $\mu\text{M}$ ) after incubating for 2 h in PBS buffer (10 mM, pH 7.4). All fluorescence spectra were obtained with the excitation at 425 nm.

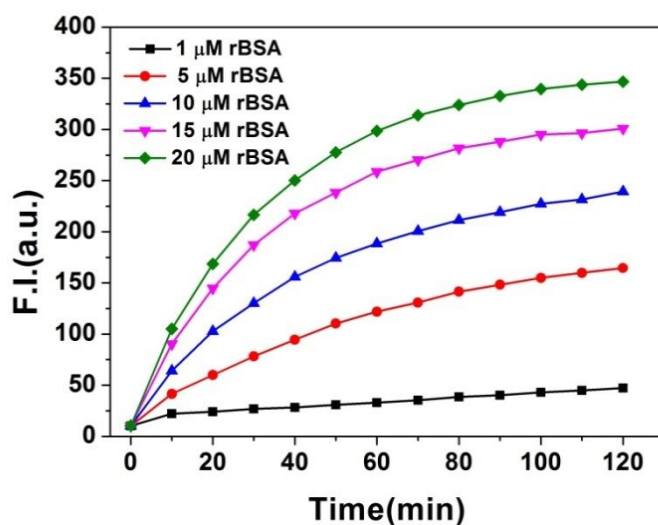


**Figure S5** Time course of the fold of fluorescence intensity increment (535 nm) of NEP (10  $\mu$ M) in the presence of different concentrations of rBSA (1, 5, 10, 15, and 20  $\mu$ M) in PBS buffer (10 mM, pH 7.4). All fluorescence spectra were obtained with the excitation at 425 nm.

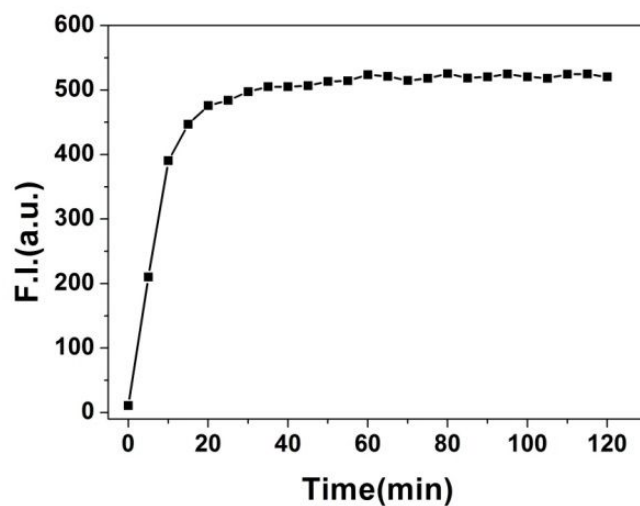


**Figure S6** Time course of the fold of fluorescence intensity increment (535 nm) of NEP (50  $\mu$ M) in the presence of DMPS (2 mM) in PBS buffer (10 mM, pH 7.4). All fluorescence spectra were obtained with the excitation at 425 nm

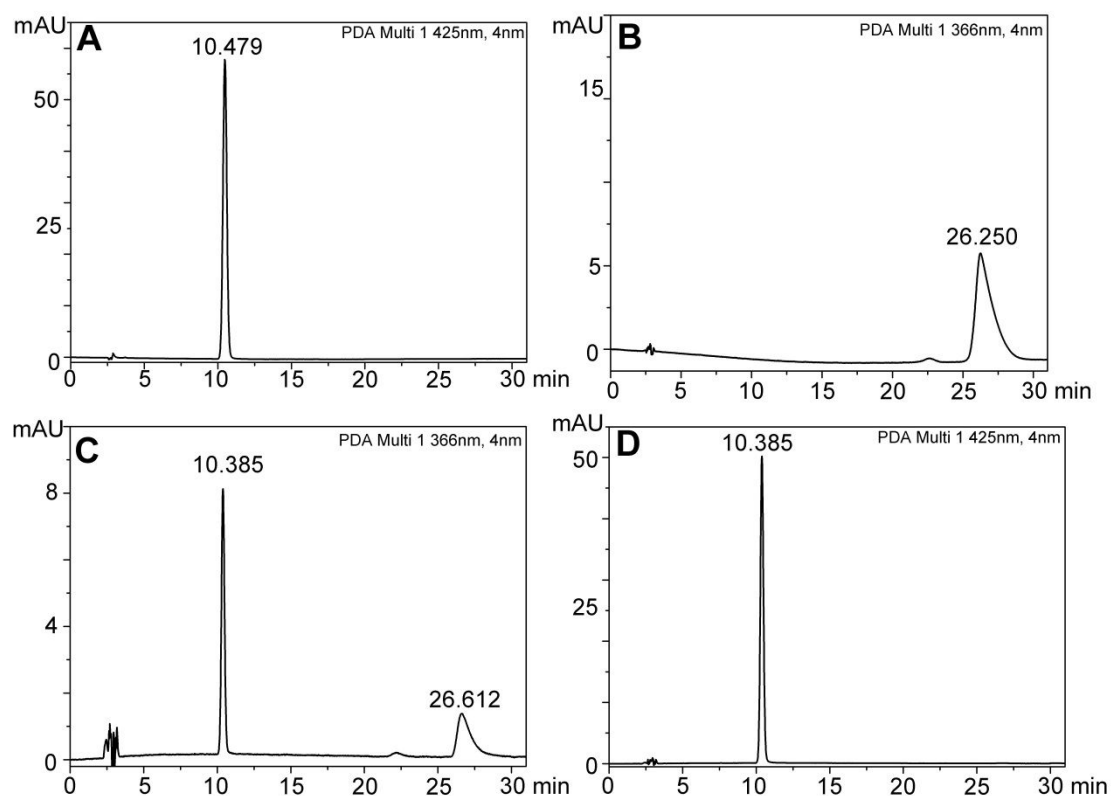


**Figure S7** HPLC analysis of the reaction of **NEP** and DMPS. (A) **Nap-NH<sub>2</sub>** (50  $\mu$ M) (425 nm); (B) **NEP** (50  $\mu$ M) (366 nm) as standard samples; (C) **NEP** (50  $\mu$ M) incubated with DMPS (2 mM) at 37  $^{\circ}$ C for 1 h in PBS buffer (366 nm); (D) **NEP** (50  $\mu$ M) incubated with DMPS (2 mM) at 37  $^{\circ}$ C for 1 h in PBS buffer (425 nm).

**Table S1.** HPLC analysis of the conversion of **NEP** activated by DMPS

<b>NEP</b>		<b>Nap-NH<sub>2</sub></b>	
Retention time: 26.250 min (425 nm)		Retention time: 10.479 min (366 nm)	
Before reaction	After 1h with DMPS	Before reaction	After 1 h with DMPS
50 $\mu$ M	2.62 $\mu$ M	0 $\mu$ M	47.15 $\mu$ M

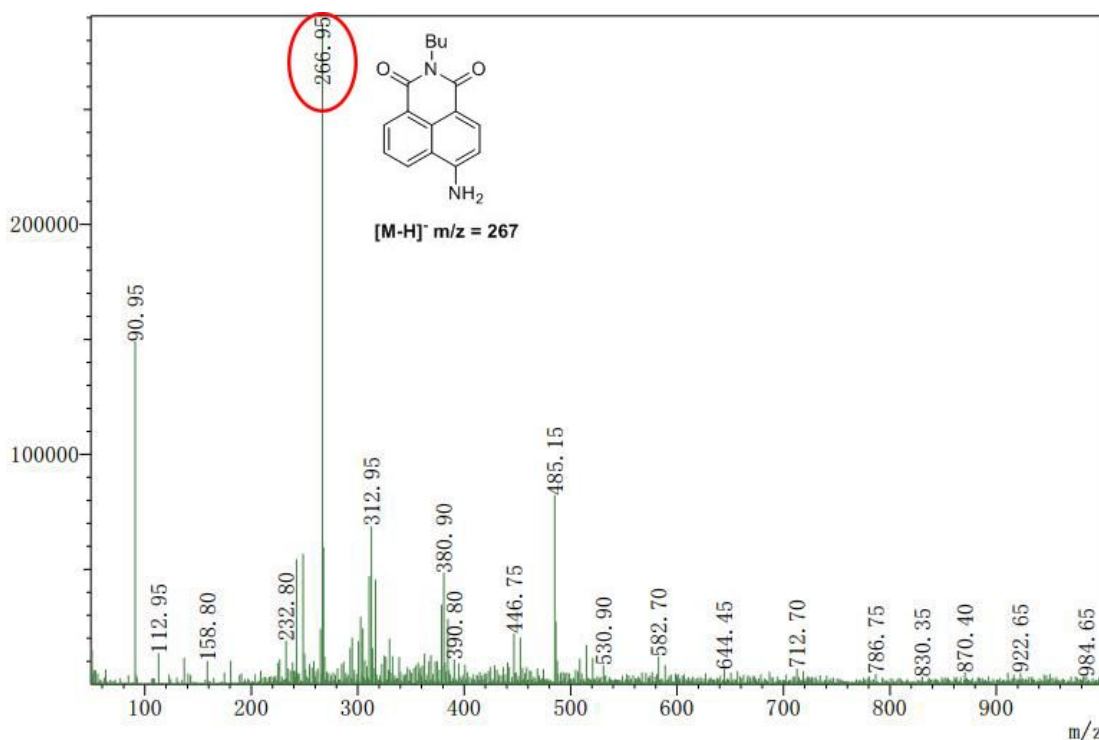


**Figure S8** Electrospray ionization mass spectrum of the reaction system that **NEP** (50  $\mu$ M) reacted with DMPS (2 mM) for 1 h in PBS buffer.

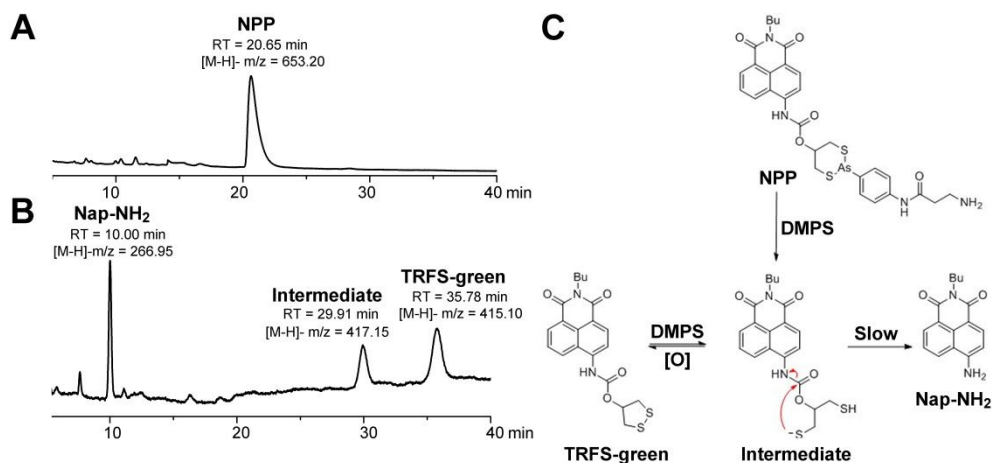


**Figure S9** Stepwise activation of **NPP** by DMPS. (A) **NPP** (25  $\mu$ M) (B) **NPP** (25  $\mu$ M) incubated with DMPS (1 mM) at 37  $^{\circ}$ C for 1 h in PBS buffer. The reaction mixture was analyzed by HPLC with a PDA detector and mass detector (MeOH/H<sub>2</sub>O=70/30, flow rate=0.6 mL/min). (C) Proposed mechanism of the activation of **NPP** by DMPS.

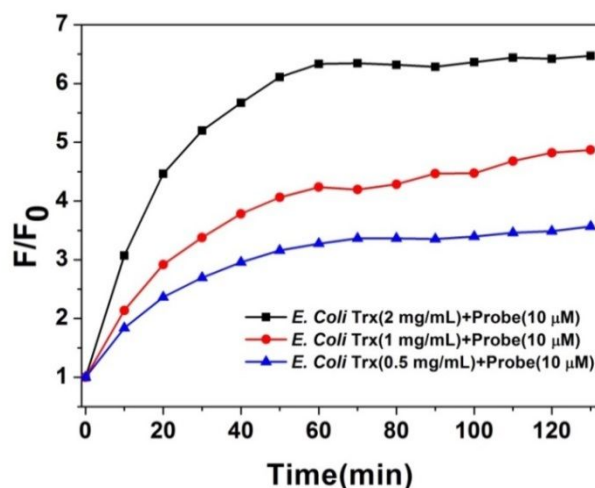


**Figure S10** Time course of the fold of fluorescence intensity increment (535 nm) of **NEP** (10  $\mu$ M) in the presence of different concentrations of reduced *E. Coli* Trx (0.5, 1, and 2 mg/mL) in PBS buffer (10 mM, pH 7.4). All fluorescence spectra were obtained with the excitation at 425 nm.

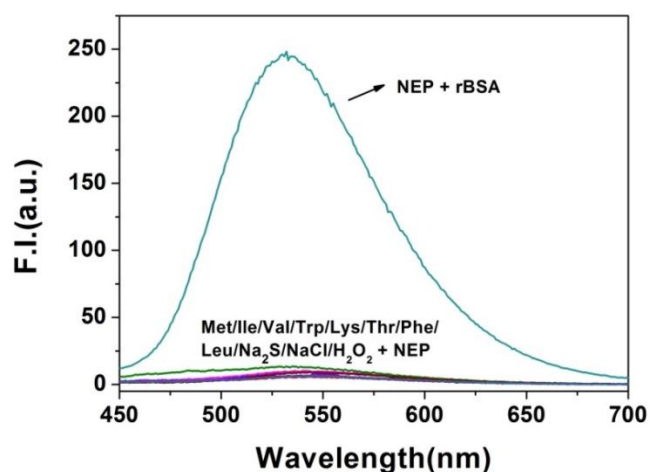


**Figure S11** Inorganic salt, common amino acids and hydrogen peroxide (1 mM) were reacted with **NEP** (10  $\mu$ M) for 2 h in PBS buffer (10 mM, pH 7.4). All fluorescence spectra were obtained with the excitation at 425 nm.

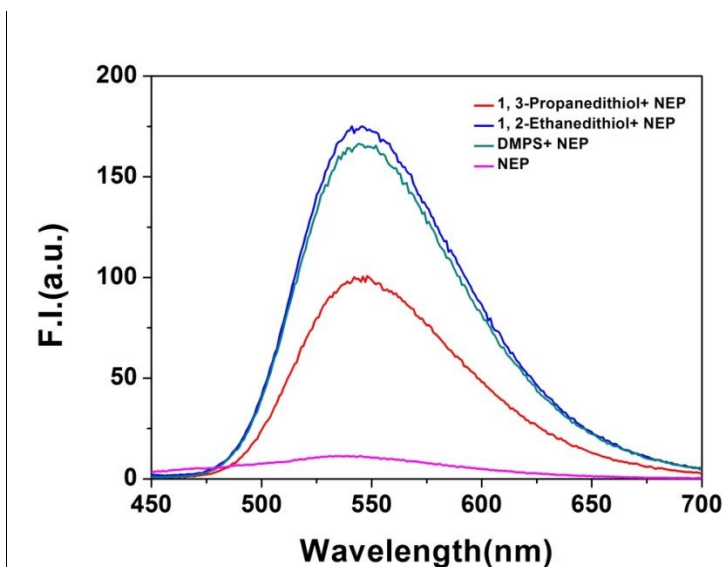


**Figure S12** low molecular weight dithiols compounds (1 mM) were reacted with **NEP** (10  $\mu$ M) for 2 h in PBS buffer (10 mM, pH 7.4). All fluorescence spectra were obtained with the excitation at 425 nm.

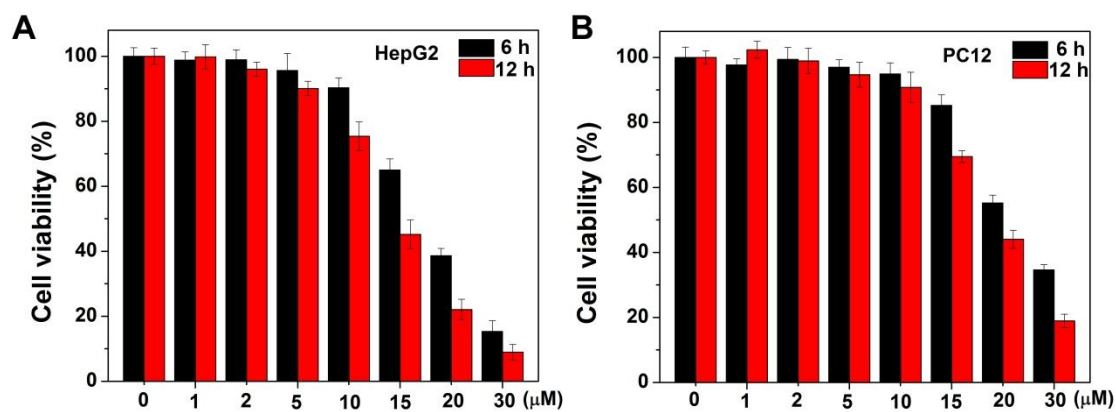


**Figure S13** Cell viability of HepG2 cells (A) and PC12 cells (B) at various concentrations of **NEP** using MTT assay.

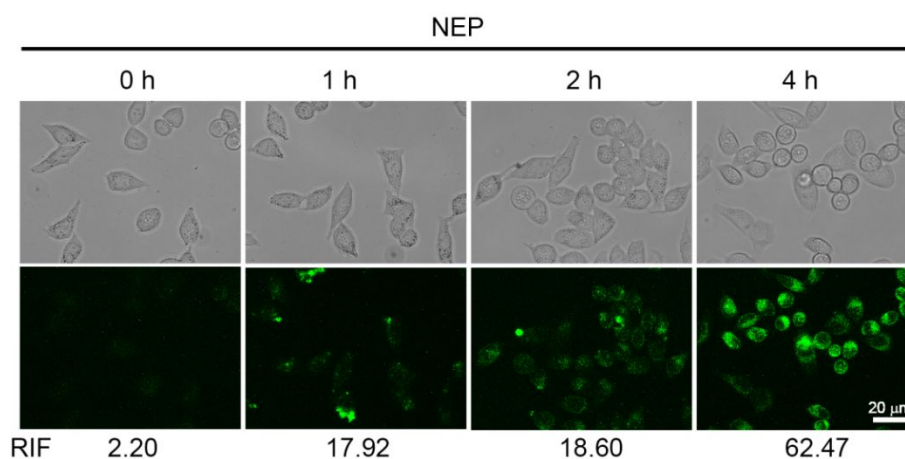


**Figure S14** Imaging VDPs in live cells. HepG2 cells treated with **NEP** (10 μM) for the indicated times, and bright field (top panel) and fluorescence (bottom panel) images were shown. Scale bar: 20 μm.

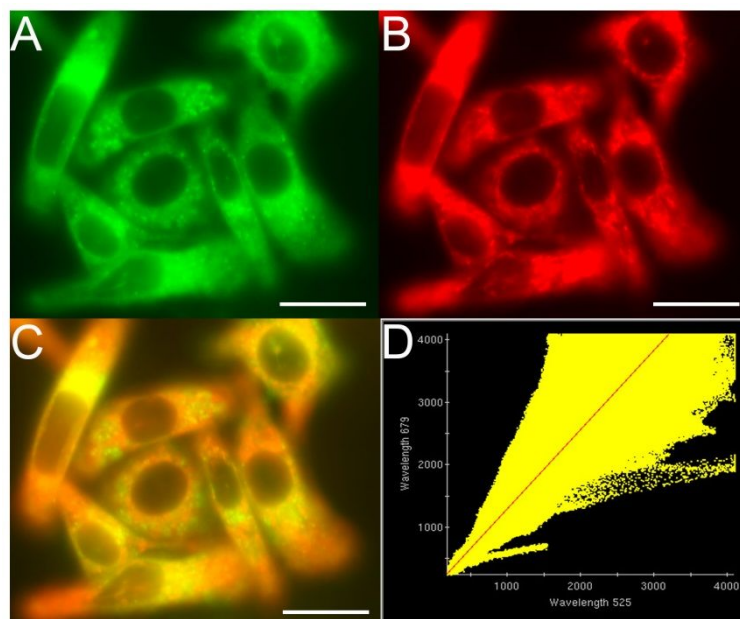


**Figure S15** Fluorescence co-localization experiments of **NEP** and Mito-Tracker Deep Red in HepG2 cells. (A) **NEP** (10  $\mu$ M) stain. Excitation:  $390\pm18$  nm. Emission collection:  $525\pm48$  nm. (B) Mito-Tracker Deep Red (50 nM) stain. Excitation:  $632\pm22$  nm. Emission collection:  $679\pm34$  nm. (C) The merged images of (A) and (B). (D) Dotplot reflected the overlay of green signal with Mito-Tracker Deep Red signal. Scale bar: 25  $\mu$ m.

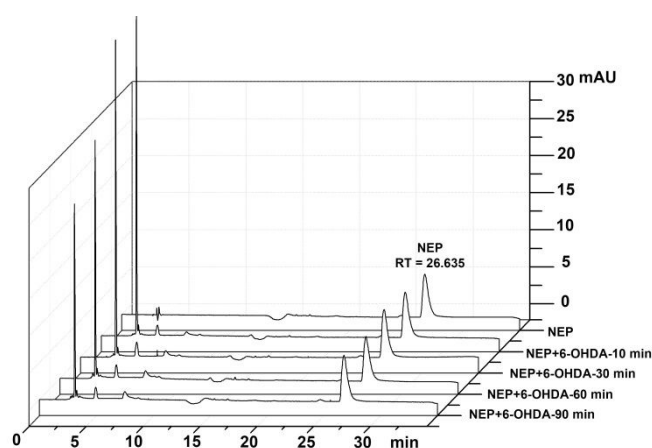


**Figure S16** NEP (10  $\mu\text{M}$ ) was incubated with 6-OHDA (200  $\mu\text{M}$ ) in PBS at 37  $^{\circ}\text{C}$ . The reaction mixture was analyzed by HPLC with a PDA detector and mass detector. Solution A: MeOH, Solution B:  $\text{H}_2\text{O}$ . Gradient elution: 1-8 min, 80% B; 8-10 min, 80-30% B; 10-30 min, 30% B; 30-35 min, 30-80% B. Flow rate=0.6 mL/min.

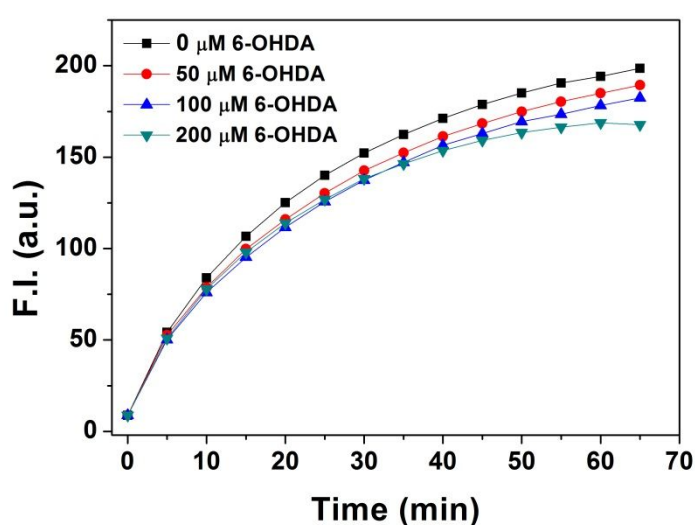


**Figure S17** Time course of the fold of fluorescence intensity increment (535 nm) of the reaction of NEP (10  $\mu\text{M}$ ) and rBSA (10  $\mu\text{M}$ ) in the presence of different concentrations of 6-OHDA (0, 50, 100, and 200  $\mu\text{M}$ ) in PBS buffer. All fluorescence spectra were obtained with the excitation at 425 nm.



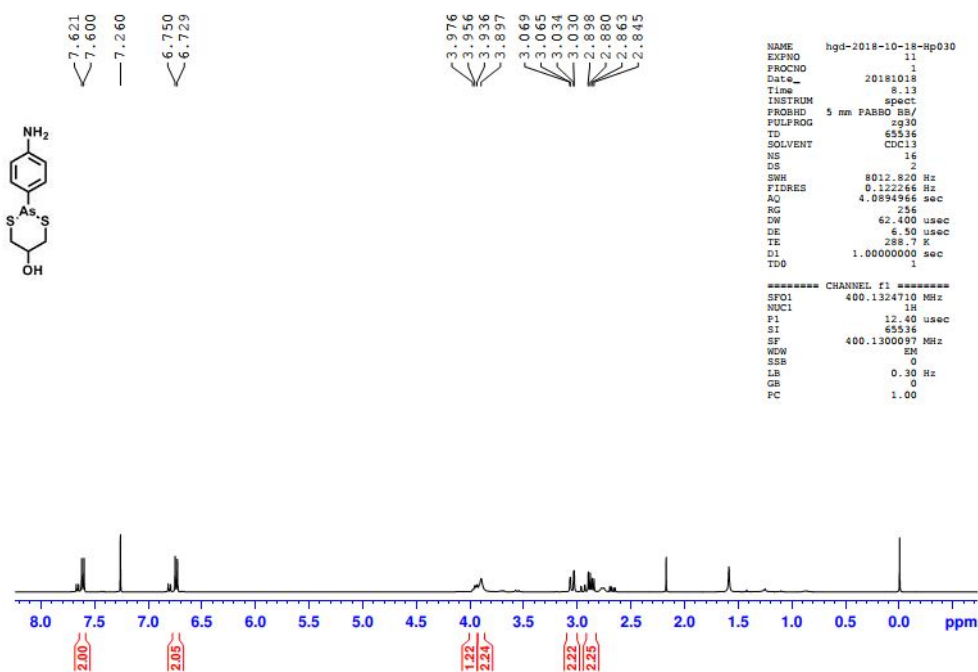


**Figure S20** <sup>1</sup>H NMR spectral of compound **2** in CDCl<sub>3</sub>

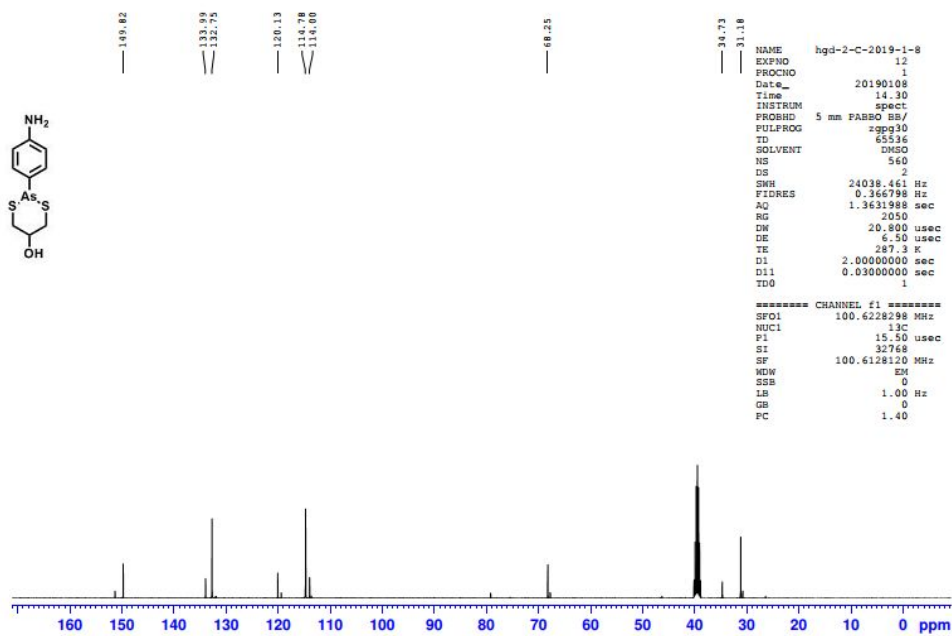


**Figure S21** <sup>13</sup>C NMR spectral of compound **2** in DMSO-d<sub>6</sub>

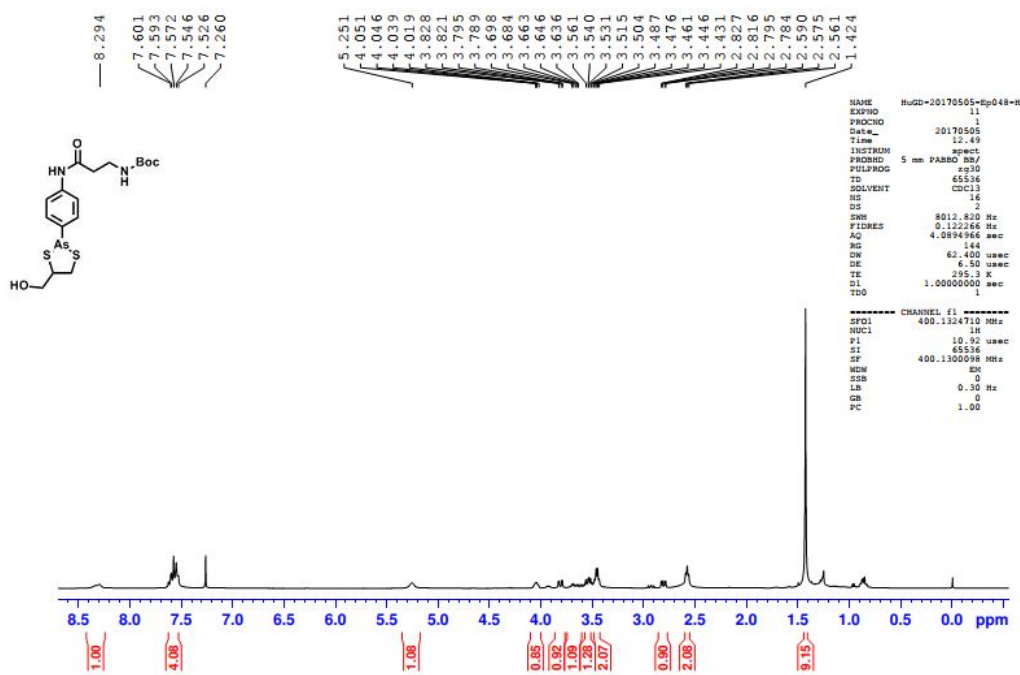


Figure S22 <sup>1</sup>H NMR spectral of compound **3** in CDCl<sub>3</sub>

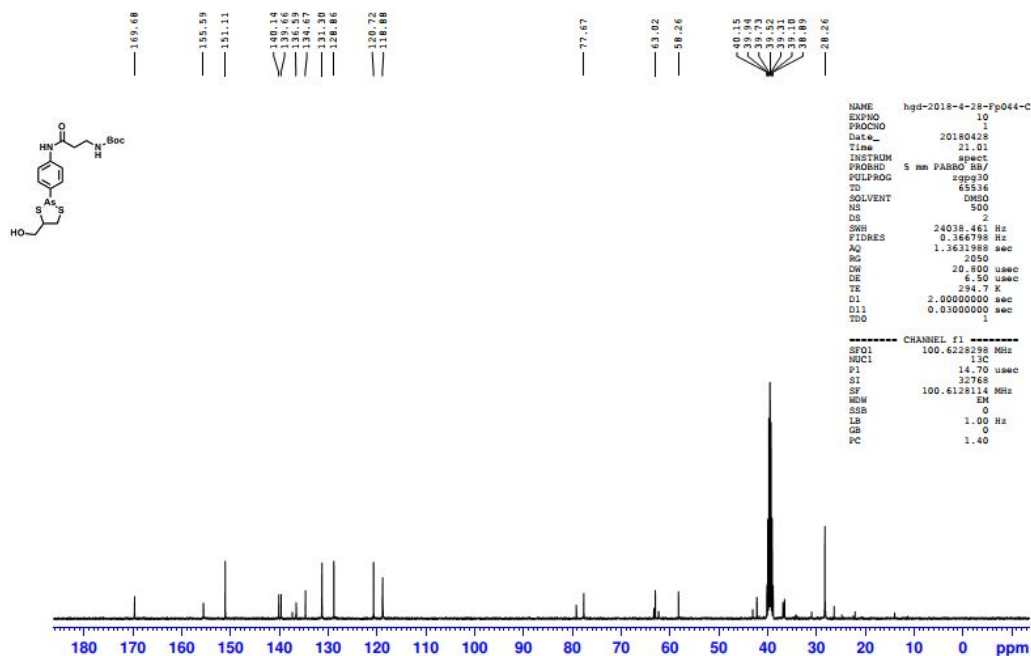


Figure S23 <sup>13</sup>C NMR spectral of compound **3** in DMSO-d<sub>6</sub>

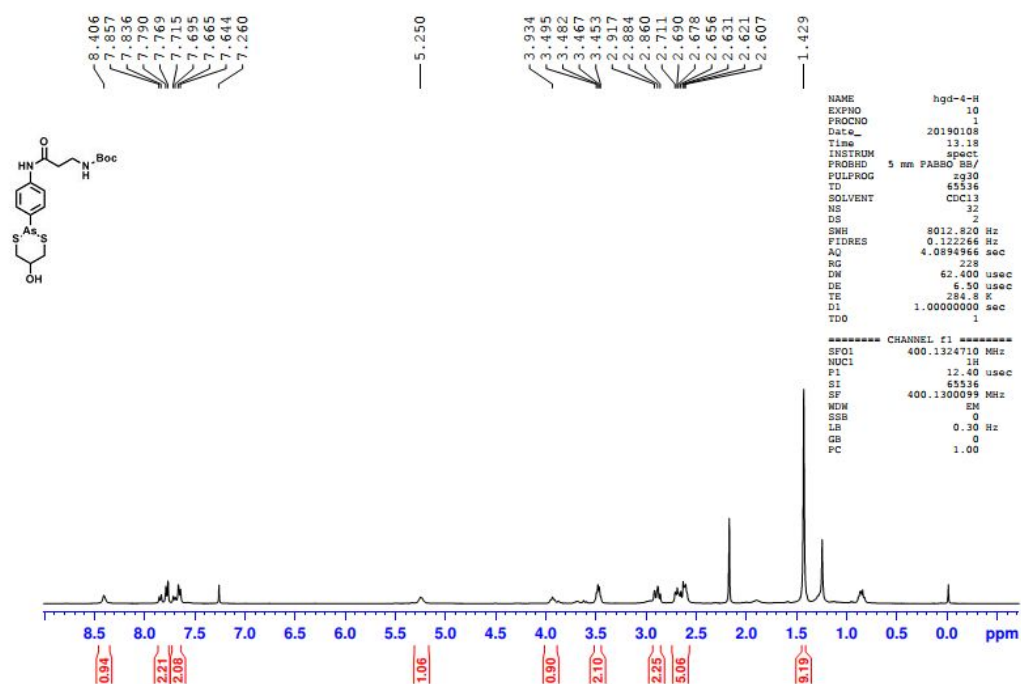


Figure S24 <sup>1</sup>H NMR spectral of compound 4 in CDCl<sub>3</sub>

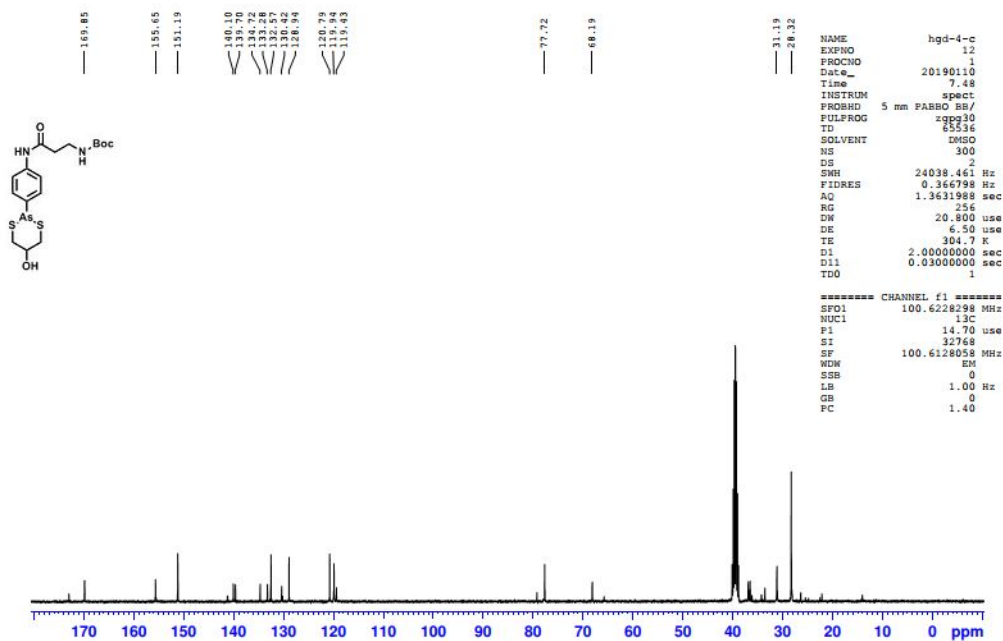


Figure S25 <sup>13</sup>C NMR spectral of compound 4 in DMSO-d<sub>6</sub>

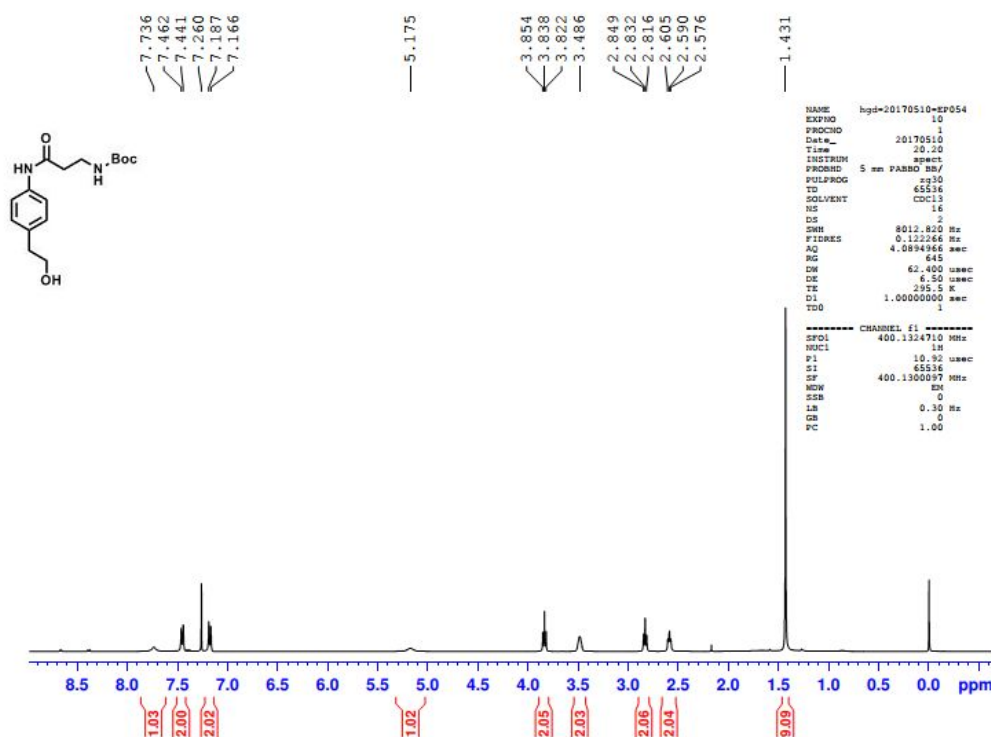


Figure S26 <sup>1</sup>H NMR spectral of compound **5** in CDCl<sub>3</sub>

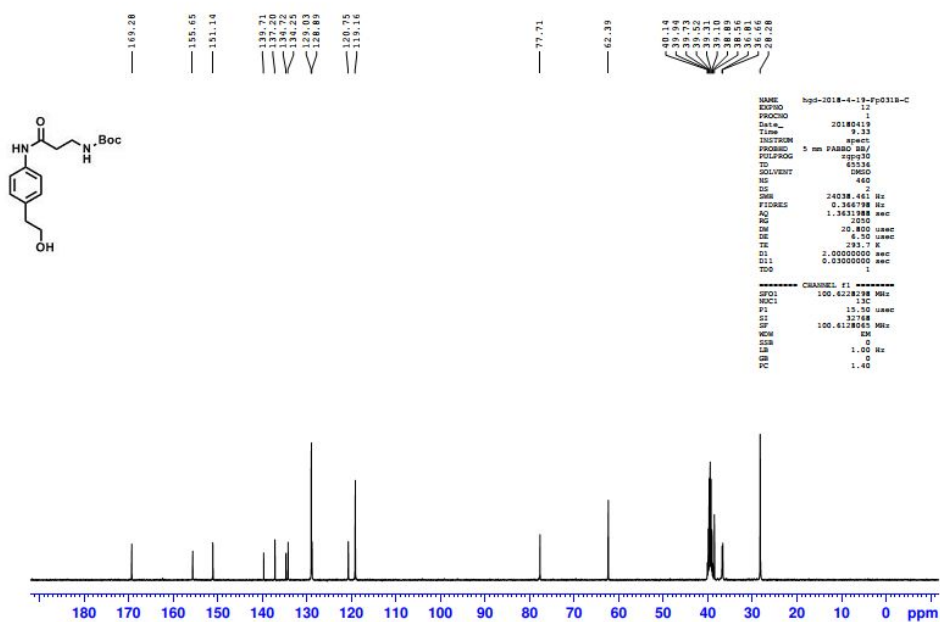
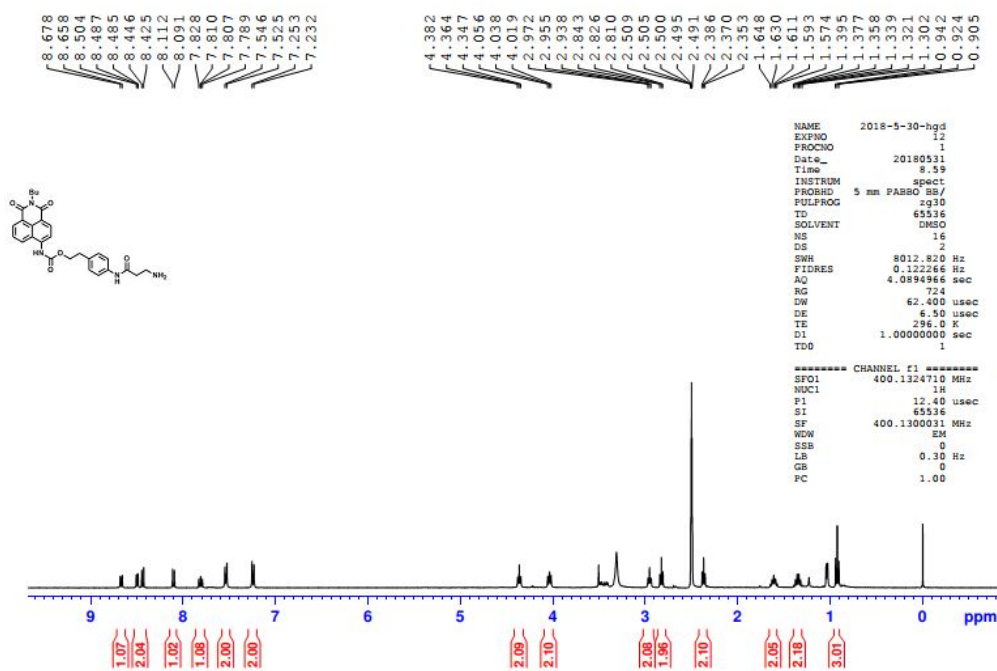
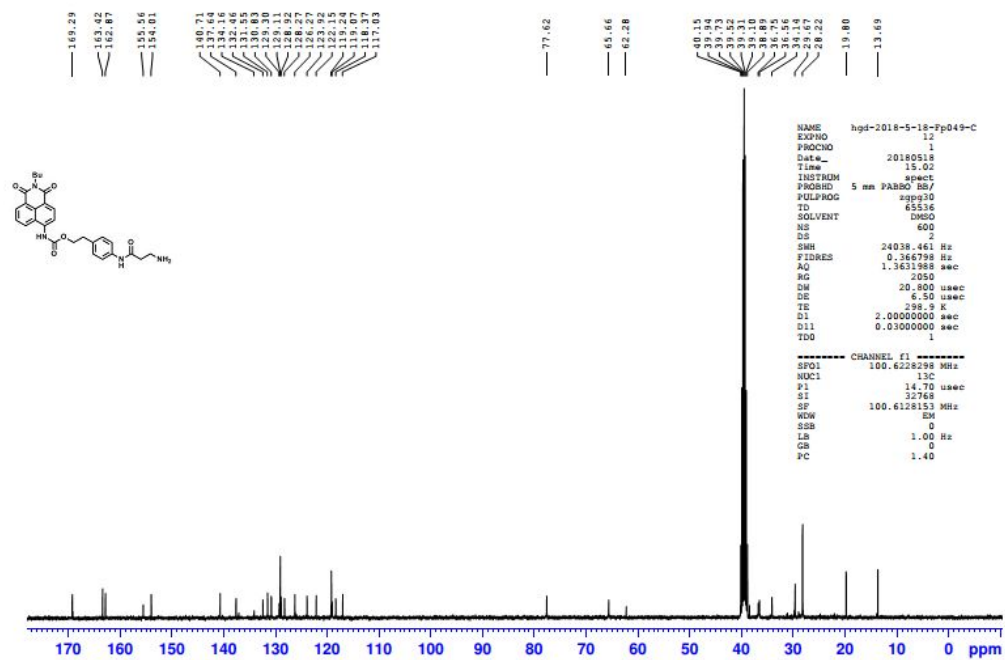


Figure S27 <sup>13</sup>C NMR spectral of compound **5** in DMSO-d<sub>6</sub>



**Figure S28** <sup>1</sup>H NMR spectral of compound NCC in DMSO-d<sub>6</sub>



**Figure S29** <sup>13</sup>C NMR spectral of compound NCC in DMSO-d<sub>6</sub>

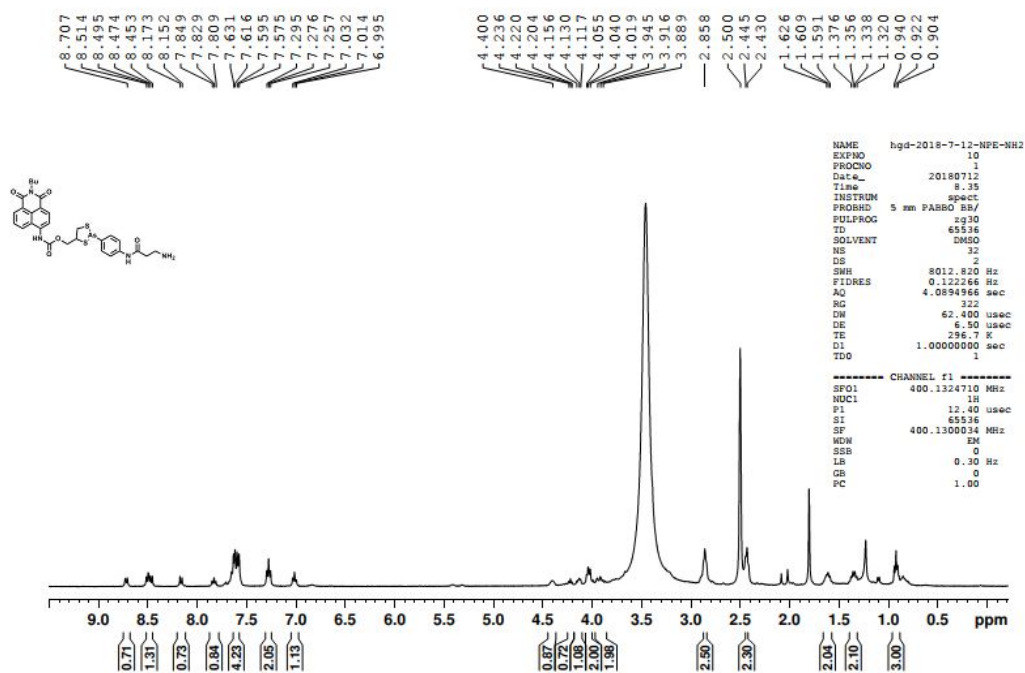


**Figure S30**  $^1\text{H}$  NMR spectral of compound **NEP** in  $\text{DMSO-d}_6$

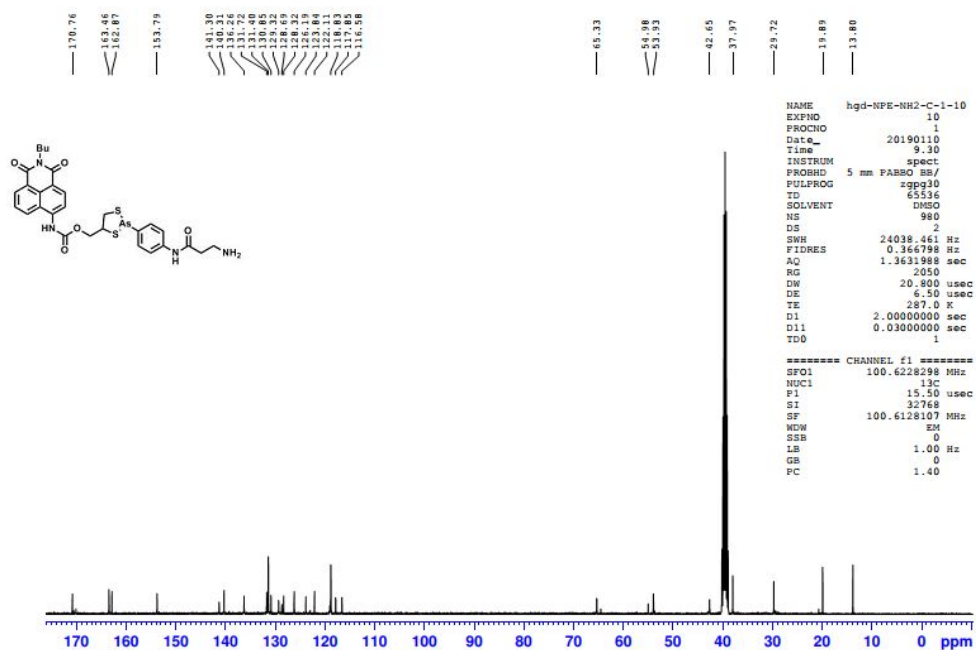


**Figure S31**  $^{13}\text{C}$  NMR spectral of compound **NEP** in  $\text{DMSO-d}_6$

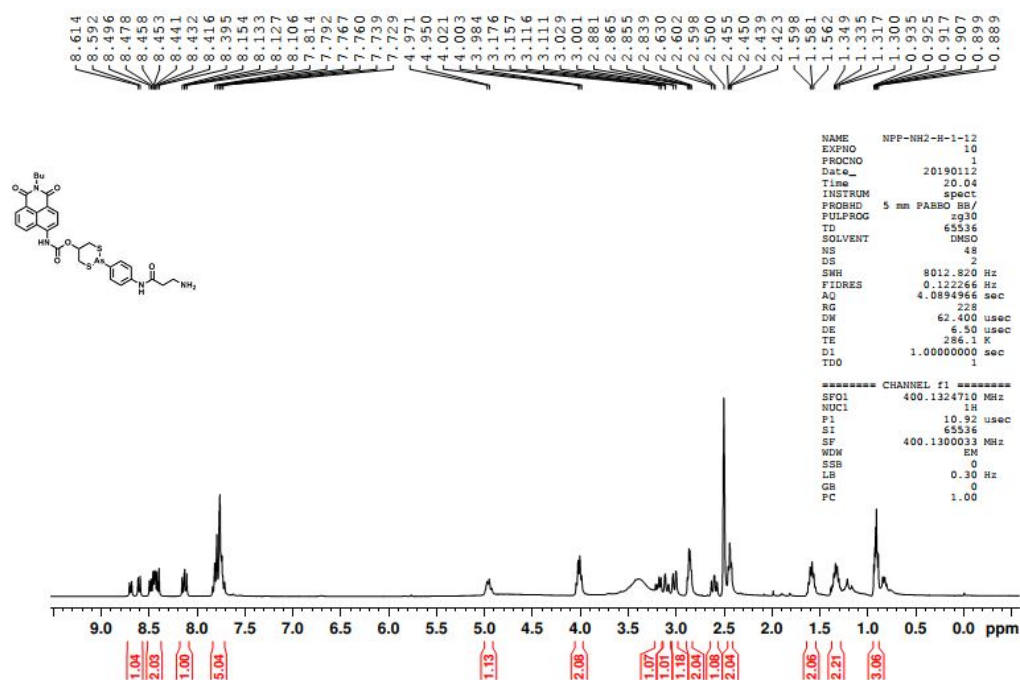


**Figure S32**  $^1\text{H}$  NMR spectral of compound **NPP** in  $\text{DMSO-d}_6$

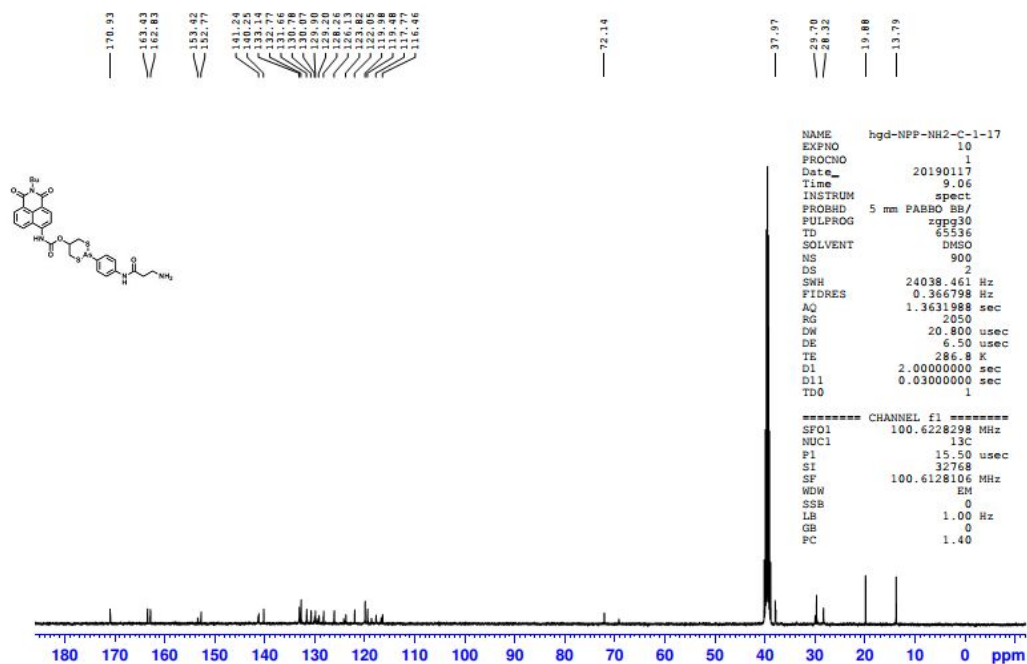


**Figure S33**  $^{13}\text{C}$  NMR spectral of compound **NPP** in  $\text{DMSO-d}_6$

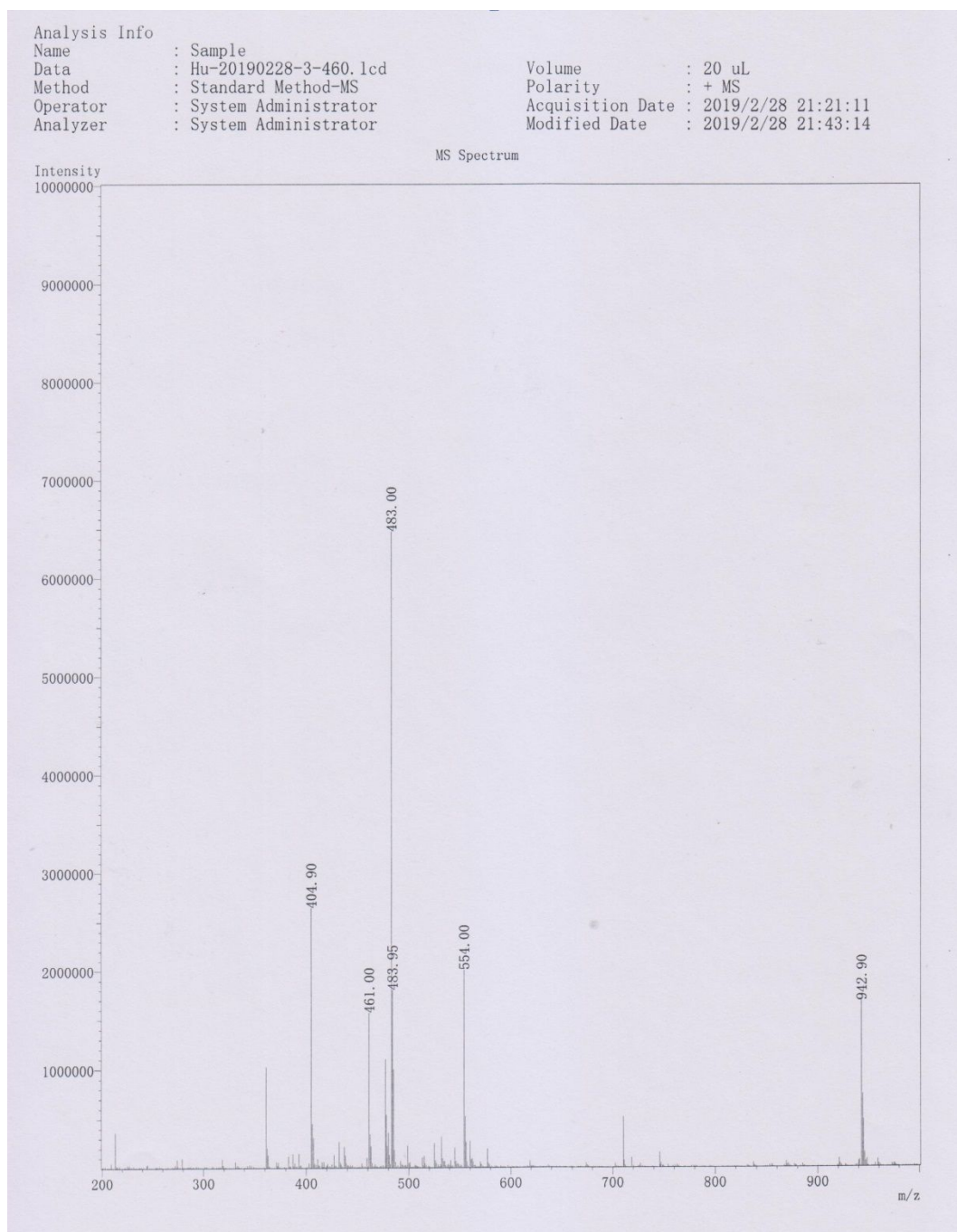


**Figure S34** Mass spectral of compound **3**

Analysis Info

Name : Sample  
Data : Hu-20190228-4-460-2.lcd  
Method : Standard Method-MS  
Operator : System Administrator  
Analyzer : System Administrator

Volume : 20  $\mu$ L  
Polarity : + MS  
Acquisition Date : 2019/2/28 16:36:18  
Modified Date : 2019/2/28 17:03:27

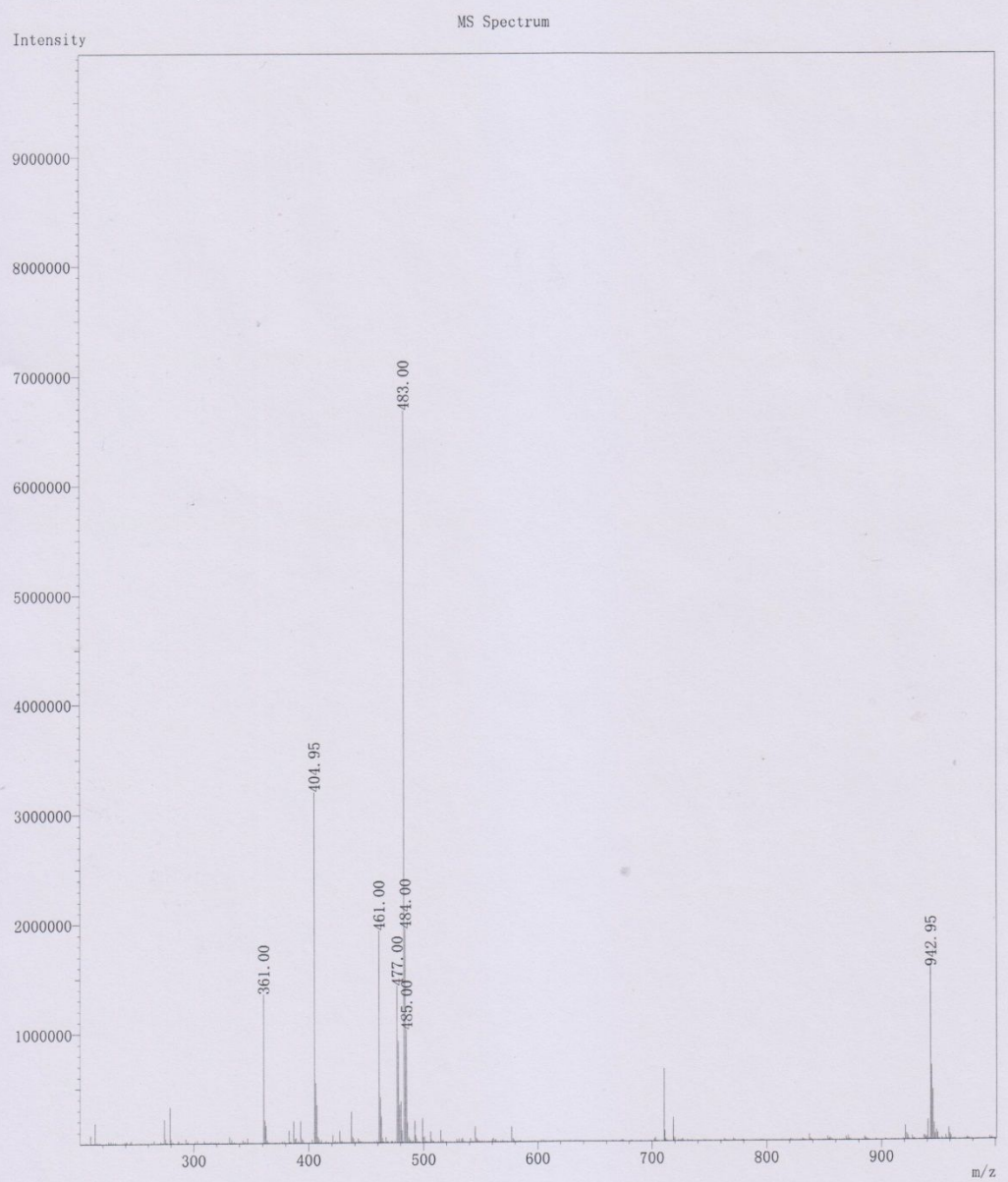


**Figure S35** Mass spectral of compound **4**

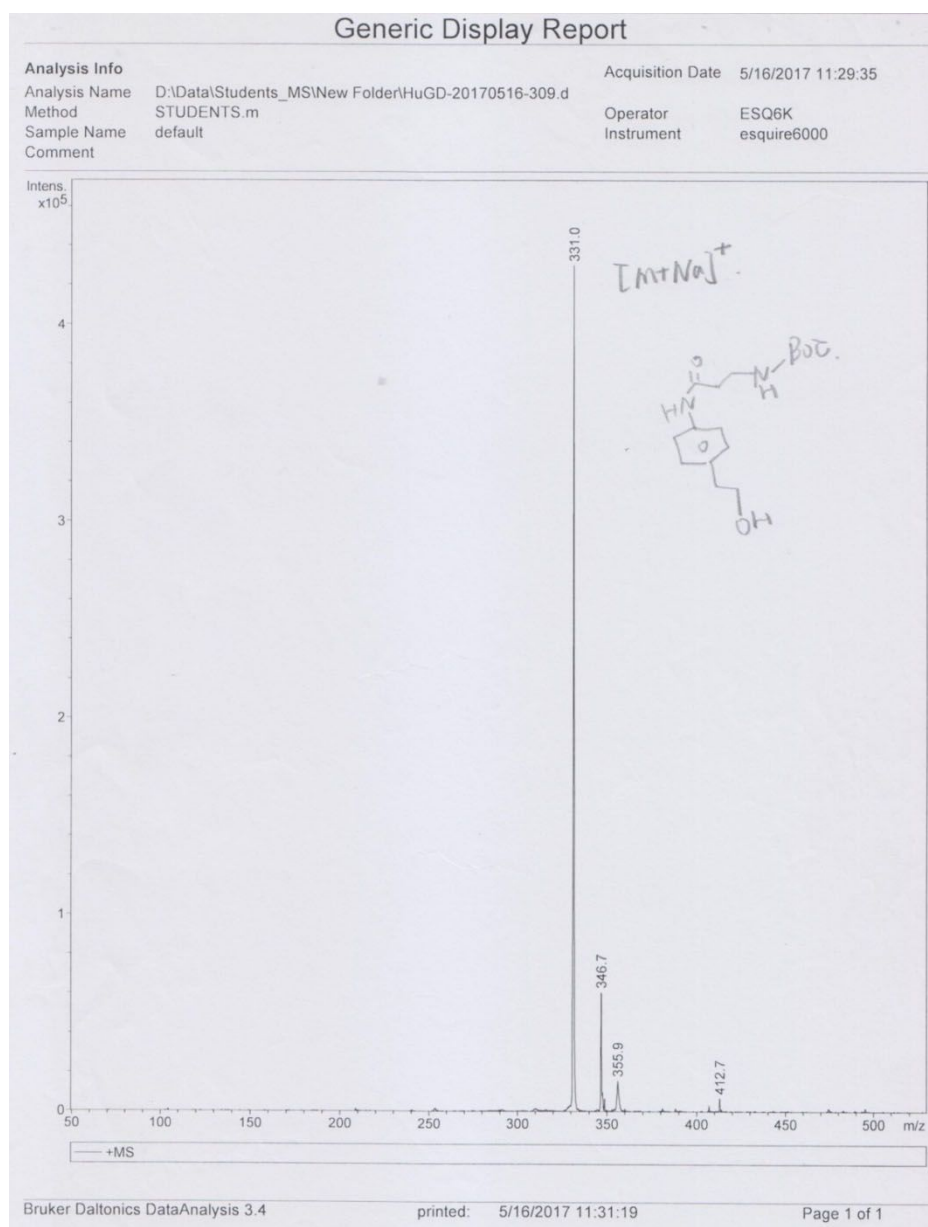
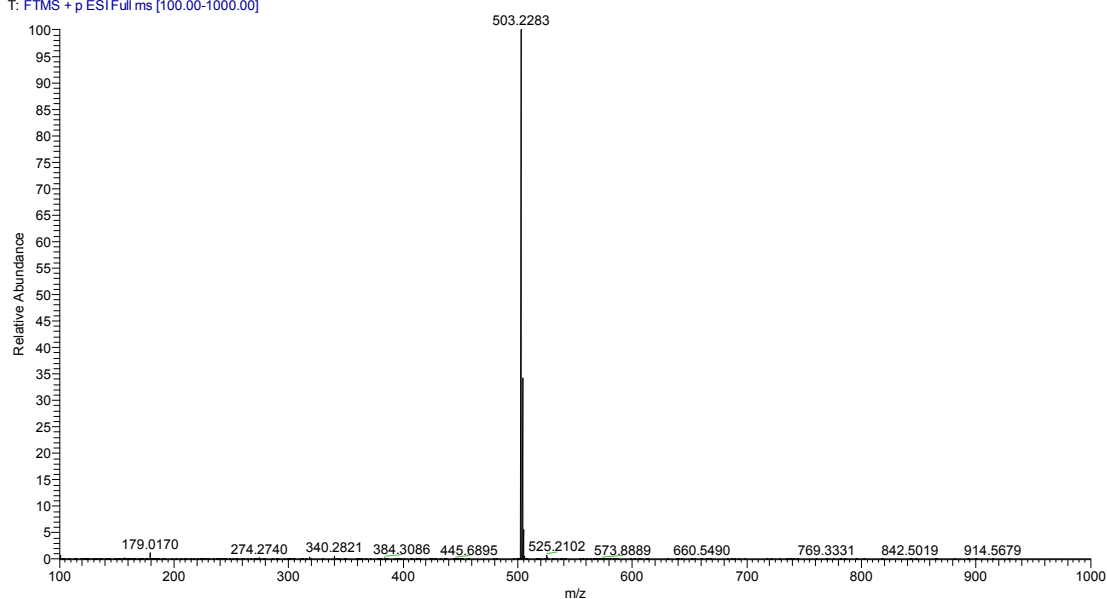


**Figure S36** Mass spectral of compound **5**

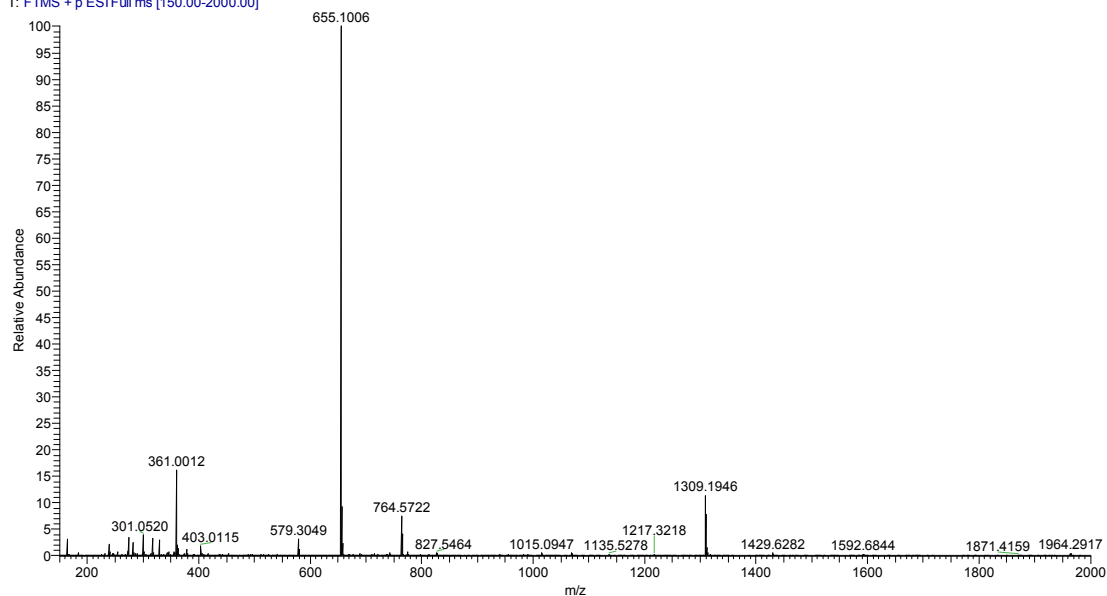
huguodong-02\_191217112401 #21 RT: 0.14 AV: 1 NL: 9.99E7  
T: FTMS + p ESI Full ms [100.00-1000.00]



m/z	Theo. Mass	Delta (mmu)	RDB equiv.	Composition
503.2283	503.2289	-0.57	15.5	C <sub>28</sub> H <sub>31</sub> O <sub>5</sub> N <sub>4</sub>

**Figure S37** High resolution mass spectral of compound **NCC**

huguodong-01\_191231153837 #1 RT: 0.00 AV: 1 NL: 2.18E7  
T: FTMS + p ESI Full ms [150.00-2000.00]



m/z	Theo. Mass	Delta (mmu)	RDB equiv.	Composition
655.1006	655.1025	-1.87	16.5	C <sub>29</sub> H <sub>32</sub> O <sub>5</sub> N <sub>4</sub> As S <sub>2</sub>

**Figure S38** High resolution mass spectral of compound **NPP**

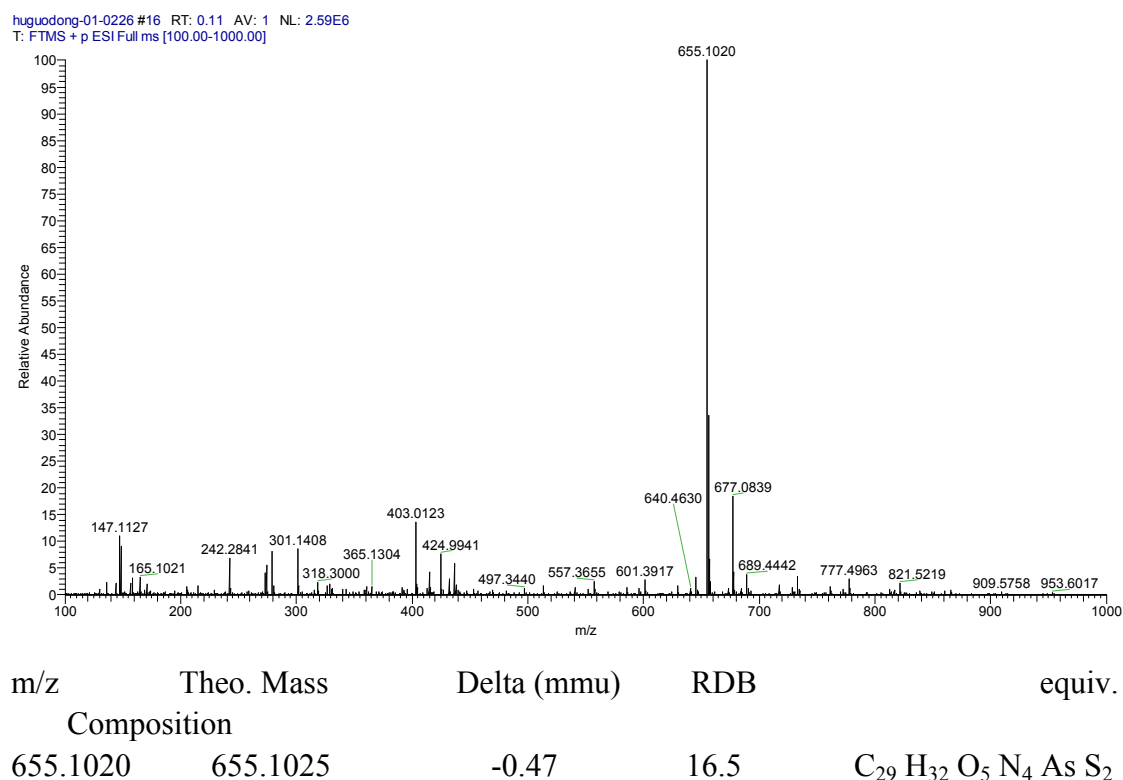


**Figure S39** High resolution mass spectral of compound **NEP**

### 3. References

- (1) Zhong, L.; Holmgren, A. Essential role of selenium in the catalytic activities of mammalian thioredoxin reductase revealed by characterization of recombinant enzymes with selenocysteine mutations. *J. Biol. Chem.*, **2000**, 275, 18121-18128.
- (2) Liu, Y.; Duan, D.; Yao, J.; Zhang, B.; Peng, S.; Ma, H.; Song, Y.; Fang, J. Dithiaarsanes induce oxidative stress-mediated apoptosis in HL-60 cells by selectively targeting thioredoxin reductase. *J. Med. Chem.*, **2014**, 57, 5203-5211.
- (3) Zhang, L.; Duan, D.; Liu, Y.; Ge, C.; Cui, X.; Sun, J.; Fang, J. Highly selective off-on fluorescent probe for imaging thioredoxin reductase in living cells. *J. Am. Chem. Soc.*, **2014**, 136, 226-233.
- (4) Heckman, K. L.; Pease, L. R. Gene splicing and mutagenesis by PCR-driven overlap extension. *Nat. Protoc.*, **2007**, 2, 924-932.
- (5) Holmgren, A.; Reichard, P. Thioredoxin 2: cleavage with cyanogen bromide. *Eur. J. Biochem.*, **1967**, 2, 187-196.
- (6) Wang, P.; Wu, J.; Di, C.; Zhou, R.; Zhang, H.; Su, P.; Xu, C.; Zhou, P.; Ge, Y.; Liu, D.; Liu, W.; Tang, Y. A novel peptide-based fluorescence chemosensor for selective imaging of hydrogen sulfide both in living cells and zebrafish. *Biosens. Bioelectron.*, **2017**, 92, 602-609.